Kazimierz MIKOŁAJUK, Andrzej TOBOŁA

Warsaw University of Technology

Ripple estimation in active power filters

Abstract. *The paper presents the analytical method of ripple estimation in active power filters. The method is based on an average model of PWM voltage source inverter. The formulae for the ripple magnitude are derived for single-phase and three-phase three-leg structures. Numerical examples for filters generating third and fifth order harmonics are presented. The example with reactive component of fundamental harmonic is considered as well.*

Streszczenie. *Przedstawiono analityczną metodę estymacji tętnienia prądu wynikającego z przełączeń obwodu w aktywnych filtrach energetycznych. Metoda opiera się na uśrednionych modelach z modulacją PWM. Odpowiednie formuły analityczne zostały opracowane dla układu jednofazowego i trójfazowego. Wykonano obliczenia dla układu generującego trzecią i piątą harmoniczną oraz układu generującego składową bierną harmonicznej podstawowej.* ***(Estymacja tętnień prądu w aktywnych filtrach energetycznych).***

Keywords: averaging techniques for switching circuits, current ripple, active power filters
Słowa kluczowe: metoda uśredniania układów przełączanych, tętnienia prądu, aktywne filtry energetyczne.

.

Introduction

An important feature of power electronic circuits working in switching scheme is a ripple effect. Switching frequency errors are undesirable effects always accompanying these techniques. Ripple errors are eliminated with the use of additional filters. Properly chosen switching algorithms can minimize the ripple effects [1]. The magnitude of current ripples can be computed by simulation of a specific PWM realisation. More general information can be obtained from analytical formulae. Such formulae can be derived when an average model of PWM inverter is employed. The averaging approximates the discontinuous system by a time-continuous model. Average models simplify analysis, make easier to understand the system's behaviour, speed up simulation and can be used for control and design purposes. The averaging method has been developed, for a wide class of power electronics circuits and has been presented in many papers. The application of averaging techniques for STATCOM and active filters has been proposed in [2].

Ripple error estimation in single-phase voltage source inverter

The deviation level of real generated current waveform from the smooth average waveform can be easy estimated for power active filters working with fixed switching frequency. The inverters working with fixed switching frequency inject harmonic components with frequency varying in narrow band.

The single-phase topology of the voltage source inverter generating desired current waveform is shown in Fig.1. A properly switched circuit should generate such current *i* that is as close to reference signal as possible. The fixed switching frequency scheme with the switching period T_S will be considered.

Let $s_1(t)$, $s_2(t)$, $s_3(t)$, $s_4(t)$ represent the on/off periodical control signals for four switching devices S_1, S_2, S_3, S_4 of the bridge inverter (Fig. 1). If the switching device is on the control signal of value 1 is assigned to it, if the switching device is off the control signal 0 is assigned to it. The constrains of these four control signals are $s_1(t)+s_2(t)=1$ and $s_3(t)+s_4(t)=1$. The resulting control signal defined as

(1) $$s(t)=s_1(t)-s_3(t)=s_4(t)-s_2(t)$$

can assume three values 1,0 and -1.

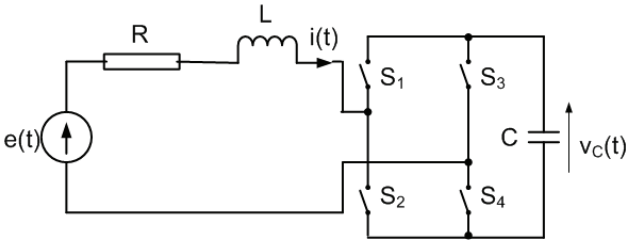

Fig. 1. Single-phase circuit generating current harmonics

When the switching system operates in open loop, the switching transitions occur at predetermined times and time function $s(t)$ takes the form of determined rectangular wave. Two modes will be considered – bipolar mode (Fig. 2a) and unipolar mode Fig.2b.

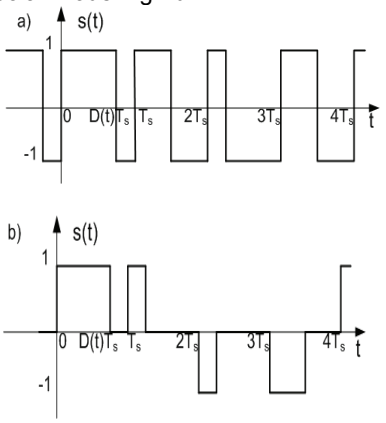

Fig.2. Switching modes: a) bipolar mode, b) unipolar mode

Function $D(t)$ means duty ratio function. Within period T_S the switching function changes as follows: for bipolar mode $s(t)=s_1=1$ for $t\in(0,D(t)T_S)$ and $s(t)=s_2=-1$ for $t\in(D(t)T_S,T_S)$; for unipolar mode $s(t)=s_1=1$ for $t\in(0,D(t)T_S)$ and $s(t)=s_2=0$ for $t\in(D(t)T_S,T_S)$.

If $i(t)$ and $\upsilon_C(t)$ are state variables, then the state equations for the time-varying circuit shown in Fig. 1 have the following form

(2) $$\frac{di(t)}{dt}=-\frac{R}{L}i(t)-\frac{1}{L}s(t)\upsilon_C(t)+\frac{1}{L}e(t)$$

(3) $$\frac{d\upsilon_C(t)}{dt}=\frac{1}{C}s(t)i(t)$$

where $s(t)$ is discontinues switching function defined in equation (1) and presented in Fig. 2.

The averaging operator within the moving interval $(t-T_S,t)$

$$\xi_{av}=\frac{1}{T_S}\int_{t-T_S}^{t}\xi(\tau)d\tau \tag{4}$$

can be applied to state equation (2) and (3) [2].

Switching period T_S is small in comparison with the periods of the harmonics to be generated by active filters. It means that variations of state variables $i(t)$ and $\upsilon_C(t)$ within interval $(t-T_S,t)$ is small and the following approximation is acceptable

$$\frac{1}{T_S}\int_{t-T_S}^{t}s(\tau)x(\tau)d\tau=s_{av}(t)x_{av}(t) \tag{5}$$

where $x(t)$ state variable, $s(t)$ discontinuous switching function, $x_{av}(t)$ average state variable and $s_{av}(t)$ average switching function.

Applying the averaging operator (4) to equations (2-3) and taking in account approximation (5), we obtain

$$\frac{di_{av}(t)}{dt}=-\frac{R}{L}i_{av}(t)-\frac{1}{L}s_{av}(t)\upsilon_{Cav}(t)+\frac{1}{L}e_{av}(t) \tag{6}$$

$$\frac{d\upsilon_{Cav}(t)}{dt}=\frac{1}{C}s_{av}(t)i_{av}(t) \tag{7}$$

Average function $s_{av}(t)$ is continuous and depends on continuous positive duty-ratio function $D(t)$ and switching mode applied in the realized control. Formula (4) applied to switching function $s(t)$ gives

$$s_{av}(t)=s_1D(t)-[1-D(t)]s_2 \tag{8}$$

Hence, for bipolar case (Fig. 2a)

$$s_{av}(t)=2D(t)-1 \tag{9}$$

and for uniplar case (Fig.2b)

$$s_{av}(t)=\pm D(t) \tag{10}$$

The sign on the right sight of equation (10) depends on polarization of switching function $s_{av}(t)$, as duty ratio function $D(t)$ is positive.

Let current $i_{av}(t)=i_{ref}(t)$ be given, then equations (6) and (7) can be reduced to one nonlinear differential equation

$$\frac{d\upsilon_{Cav}(t)}{dt}=f_1(t)f_2(t)\frac{1}{\upsilon_{Cav}(t)} \tag{11}$$

where

$$f_1(t)=-L\frac{di_{ref}(t)}{dt}-Ri_{ref}(t)+e_{av}(t),\ f_2(t)=\frac{1}{C}i_{ref}(t) \tag{12}$$

Solving the Bernoullie type equation (11) with capacitor voltage $\upsilon_{Cav}(t)>0$, the average switching function can be obtained

$$s_{av}(t)=\frac{f_1(t)}{\upsilon_{Cav}(t)} \tag{13}$$

and duty-ratio function $D(t)$ can be computed from equation (9) or (10). According to Fig. 2b for unipolar mode $s_1=\pm1$, $s_2=0$. If voltage $\upsilon(t)=f_1(t)$ given in (12) is positive then $s_1=1$, if this voltage is negative then $s_1=-1$.

Actual current waveform $i(t)$ differs from smooth averaged current $i_{av}(t)$, it contains ripples caused by switching. To analyze the ripple within *k*th switching step, the short time interval $t\in(t_k,t_k+T_S)$ containing single switching period will be considered. Two switching are performed within period T_S at $t=t_k$ and $t=t_k+DT_S$, where $D=D(t_k)$.

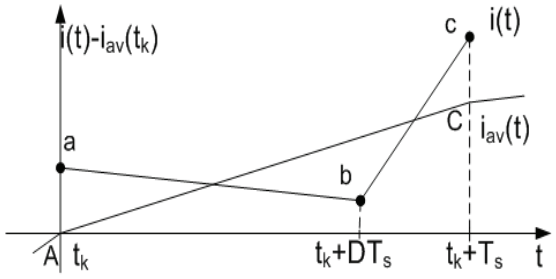

Fig. 3. Piece wise linear approximation of average and actual current within one switching period

The approximated piece wise linear waveforms of averaged current $i_{av}(t)$ and actual rippled current $i(t)$ are shown in Fig.3. The segment *AC* represents the linear approximation of the waveform $i_{av}(t)$ under the following assumptions: for $t\in(t_k,t_k+T_S)$

$e_{av}(t)=e(t_k)$, $\upsilon_{Cav}(t)=\upsilon_C(t_k)$, $s_{av}(t)=s_{av}(t_k)$.

Similarly the segments *ab* and *bc* represent piece wise linear approximations of the waveform $i(t)$ under the following assumptions:

$e(t)=e(t_k)$, $\upsilon_C(t)=\upsilon_C(t_k)$ for $t\in(t_k,t_k+T_S)$ and $s(t)=s_1=s_1(t_k)$

for $t\in(t_k,t_k+DT_S)$, $s(t)=s_2=s_2(t_k+DT_S)$

for $t\in(t_k+DT_S,t_k+T_S)$.

Additionally for both waveforms the resistance R is omitted, $R=0$. The piece-line segments *abc* represent rippled waveform only within the analyzed switching period. The segment in the next period do not need to be continues at $t=t_k+T_S$, although the actual current $i(t)$ is continues.

Under such assumptions the equation of the line segment *AC* can be obtained from (6)

$$i_{av}(t)=\frac{1}{L}[e(t_k)-s_{av}(t_k)\upsilon_C(t_k)](t-t_k)+i_{av}(t_k) \tag{14}$$

Similarly the equations of line segments *ab* and *bc* can be obtained from (2) and we have respectively

$$i(t)=\frac{1}{L}[e(t_k)-s_1\upsilon_C(t_k)](t-t_k)+i(t_k) \tag{15}$$

$$i(t)=\frac{1}{L}\{[e(t_k)-s_2\upsilon_C(t_k)](t-t_k)-(s_1-s_2)\upsilon_C(t_k)DT_S\}+i(t_k) \tag{16}$$

where $D=D_k$ and $s_1=s_{1k}, s_2=s_{2k}$ duty-ratio and switching functions for *k*th switching step.

Ripple function $\Delta i(t)$ can be defined as difference between actual current $i(t)$ and average current $i_{av}(t)$

$$\Delta i(t)=i(t)-i_{av}(t) \tag{17}$$

Substituting (14) and (15) or (16) into (17) gives

$$\Delta i(t)=\frac{1}{L}[-s_1+s_{av}(t_k)]\upsilon_C(t_k)(t-t_k)+i(t_k)-i_{av}(t_k) \tag{18}$$

for $t\in(t_k,t_k+DT_S)$ and

$$\Delta i(t)=\frac{1}{L}\{[-s_2+s_{av}(t_k)]\upsilon_C(t_k)(t-t_k)-(s_1-s_2)\upsilon_C(t_k)DT_S\}+i(t_k)-i_{av}(t_k) \tag{19}$$

for $t\in(t_k+DT_S,t_k+T_S)$.

The average value of the ripple function is equal zero

$\int_{t_k}^{t_k+T_s} \Delta i(t)dt = 0$. Applying this condition to functions (18) and (19) the ripple magnitude $\Delta i(t_k) = i(t_k) - i_{av}(t_k)$ can be obtained

$$\Delta i(t_k) = \frac{\upsilon_C T_s}{2L}[(s_1 - s_{av}(t_k))(D_1^2 + 2D_1D_2) + (s_2 - s_{av}(t_k))D_2^2] \quad (20)$$

where $D_1 = D$, $D_2 = 1 - D$ and $D = D(t_k) = \frac{s_{av}(t_k) - s_2}{s_1 - s_2}$

The piece wise linear current shown in Fig. 3 fulfils constrains $\Delta i(t_k) = \Delta i(t_k + T_s)$ and $\Delta i(t_k) = -\Delta i(t_k + DT_s)$.

The ripple magnitude is obtained (20) can be rewritten as

$$\Delta i(t_k) = -\Delta i(t_k + DT_s) = \frac{\upsilon_C(t_k)T_s}{L}(1-D)D \quad (21)$$

for bipolar mode and

$$\Delta i(t_k) = -\Delta i(t_k + DT_s) = \frac{\upsilon_C(t_k)T_s}{2L}(1-D)D \quad (22)$$

for unipolar mode

Duty ratio *D* can be substituted for average switching function $s_{av}(t_k)$ (20) and then (21), (22) take the form

$$\left|\Delta i(t_k)\right| = \left|-\Delta i(t_k + DT_s)\right| = \frac{\upsilon_C(t_k)T_s}{4L}[1 - s_{av}(t_k)][1 + s_{av}(t_k)] \quad (23)$$

for bipolar mode, and

$$\left|\Delta i(t_k)\right| = \left|-\Delta i(t_k + DT_s)\right| = \frac{\upsilon_C(t_k)T_s}{2L}[1 - \left|s_{av}(t_k)\right|]\left|s_{av}(t_k)\right| \quad (24)$$

for unipolar mode.

Example 1 – third order harmonic generation
Assume that third order current harmonic should be generated in the switched circuit shown in Fig. 1.

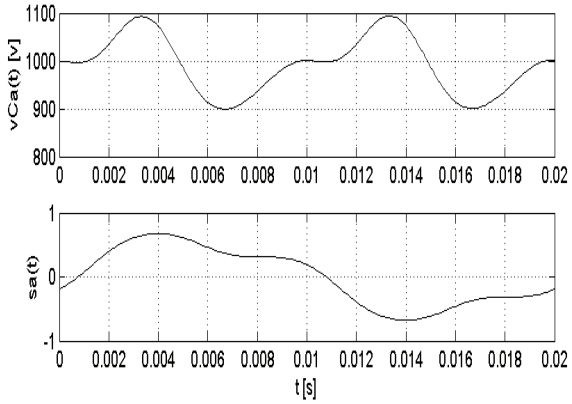

Fig. 4. Average capacitor voltage and average switching function

The results have been obtained for the following circuit parameters: $e(t) = 600\sin(314t)$, $L = 10$ mH, $R = 0.08\Omega$, $C = 128.2\mu$F, capacitor conductance *G*=0.00013S and switching period $T_s = 0.1$ ms. The assumed current to be generated is $i(t) = i_{ref}(t) = 20\sin(3 \cdot 314t) + 0.1\sin(314t)$ .The small first order current has to be added in order to ensure the energy balance. Capacitance voltage $\upsilon_{Cav}(t)$ and average switching function $s_{av}(t)$ have been computed from equations (11) and (14) with initial condition $\upsilon_{Cav}(0) = 1000V$. The results are shown in Fig. 4.

The ripple magnitude for unipolar and bipolar modes computed from equations (25) and (26) and are shown in Fig. 5.

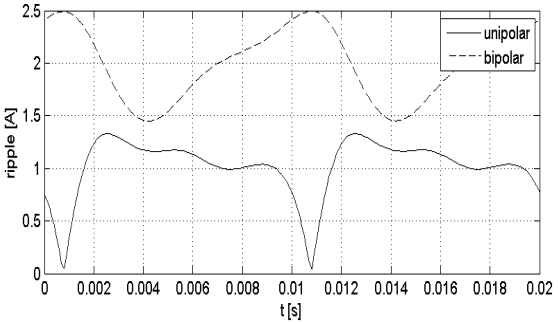

Fig. 5. Ripples for unipolar and bipolar modes

Example 2 – reactive fundamental harmonic generation
The source voltage is sinusoidal $e(t) = 600\sin(314t)$, and current $i_a(t) = 200\cos\omega t + 5.34\sin\omega t$ should be generated. The circuit parameters *L,C,R,* initial capacitor voltage $\upsilon_{Cav}(0)$ and switching period T_s have been chosen the same as in *Example 1.* Capacitor voltage $\upsilon_{Cav}(t)$ and average switching function $s_{av}(t)$ are shown in Fig. 6.

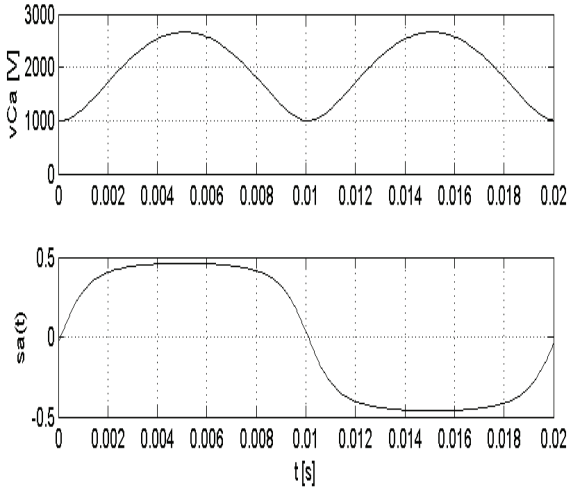

Fig. 6. Average capacitor voltage and average switching function

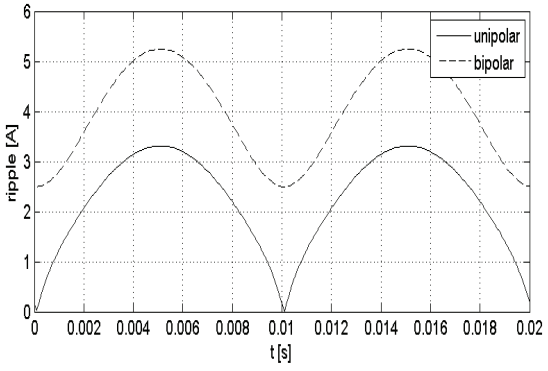

Fig.7. Ripple magnitude for unipolar and bipolar modes

The ripple magnitude for unipolar and bipolar modes obtained from equations (25) and (26) are shown in Fig. 7. It can be observed in Fig. 5 and 7 that in both examples the

ripple magnitude is smaller for unipolar mode than for bipolar mode. Such relation is valid within the whole time interval.

Ripple error in three-phase voltage source inverter

The three-phase three-leg topology of the voltage source inverter generating desired current waveform is shown in Fig.8. PWM strategies based on the concept of voltage space vectors is considered in the paper. The ripple of line current can be estimated similarly like in the single-phase inverter presented above.

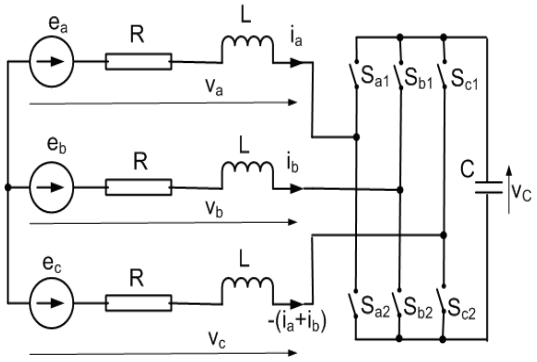

Fig. 8. Three-phase three-leg switched circuit generating current harmonics

The diagram of voltage space vector , corresponding to the eight available logic states of the inverter, is shown in Fig. 9.

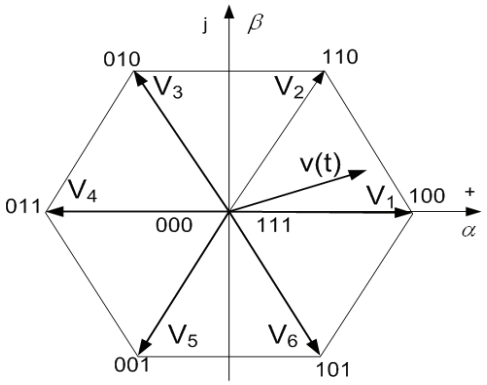

Fig. 9. The space vector diagram

There are six non-zero vectors and two zero vectors. The complex form of the two dimensional space vector is a function of the number of inverter logic state n , and can be written as follows

(25) $\underline{V_n} = V_{\alpha n} + jV_{\beta n} = \frac{2}{3}V_{Cav}(t)e^{j\frac{(n-1)\pi}{3}}$ for $n = 1,..6$

Each logic state n responds to the state of phase switches as shown in the table below

n	1	2	3	4	5	6
$s_{a1}s_{b1}s_{c1}$	100	110	010	011	001	101

Magnitudes of voltage vectors are expressed in relation to the average capacitor voltage $\upsilon_{Cav}(t)$. For simulation purpose the capacitor voltage can be computed from power balance of the inverter. For given reference currents $i_{aav} = i_{aref}$ $i_{bav} = i_{bref}$ capacitor voltage V_{Cav} can be predicted and the phase voltages are also known

(26) $\upsilon_{pav} = e_{pav} - L\frac{di_{pref}}{dt} - Ri_{pref}$ for $p = a, b.c$

The orthogonal components of these voltages can be expressed in a complex form

(27) $\underline{\upsilon_{av}} = \upsilon_{\alpha av} + j\upsilon_{\beta av}$

where

(28) $\begin{bmatrix} \upsilon_{\alpha av} \\ \upsilon_{\beta av} \end{bmatrix} = \frac{1}{3}\begin{bmatrix} 2 & -1 & -1 \\ 0 & \sqrt{3} & -\sqrt{3} \end{bmatrix}\begin{bmatrix} \upsilon_{aav} \\ \upsilon_{bav} \\ \upsilon_{cav} \end{bmatrix}$

The average switching function defined according to (4) and (5) can be obtained in similar way as shown in (14) for single phase case

(29) $s_{pav}(t_k) = \frac{3\upsilon_{pav}(t_k)}{2V_{Cav}(t_k)}$ for $p = \alpha, \beta$

In a given switching interval any vector $\underline{\upsilon_{av}}$ confined within the hexagon linking the ends of the non-zero vectors can be realized as a linear combination of the two adjacent non-zero vectors $\underline{V_n}$, $\underline{V_{n+1}}$ and either one of two zero vectors. Coefficients of this combination constitute duty ratios of the inverter states generating the employed three vectors.

Let actual vector $\underline{\upsilon}$ be placed between two adjacent vectors $\underline{V_n}$ and $\underline{V_{n+1}}$ for $n = 1,...,6$. The actual vector $\underline{\upsilon}$ is realized as linear combination

(30) $D_1\underline{V_n} + D_2\underline{V_{n+1}} = \underline{\upsilon_{av}}$

where D_1 and D_2 real numbers equal to the duty ratios associated with vector $\underline{V_n}$ and $\underline{V_{n+1}}$, respectively. The remaining duty ratio $D_{3n} = 1 - D_{1n} - D_{2n}$ is associated with either one of two zero vectors.

Taking into account equation (29), (37) and (30), we obtain

(31) $\begin{bmatrix} D_{1n} \\ D_{2n} \end{bmatrix} = \frac{\sqrt{3}}{V_C}\begin{bmatrix} \sin\frac{n\pi}{3} & -\cos\frac{n\pi}{3} \\ -\sin\frac{(n-1)\pi}{3} & \cos\frac{(n-1)\pi}{3} \end{bmatrix}\begin{bmatrix} \upsilon_\alpha \\ \upsilon_\beta \end{bmatrix}$ $n = 1,...,6$

Therefore, in a given switching period T_s respected to *n*th sector of vector space there are three subintervals with no switching inside them. If the beginning of the considered switching period is t_k , then the subintervals are: $(t_k, t_k + D_{1n}T_s)$, $(t_k + D_{1n}T_s, t_k + (D_{1n} + D_{2n})T_s)$ and $(t_k + (D_{1n} + D_{2n})T_s, t_k + T_s)$.

Discontinues switching functions s_{1n} , s_{2n} and s_{3n} are associated with these three intervals. These functions result from (25)

(32) $s_{1n\alpha} = \cos\frac{(n-1)\pi}{3}$, $s_{2n\alpha} = \cos\frac{n\pi}{3}$

(33) $s_{1n\beta} = \sin\frac{(n-1)\pi}{3}$, $s_{2n\beta} = \sin\frac{n\pi}{3}$

and $s_{3n\alpha} = s_{3n\beta} = 0$ for $n = 1,...,6$.

Respecting the assumptions introduced for the single-phase case, the piece wise linear current of chosen phase can be depicted as in Fig. 10.

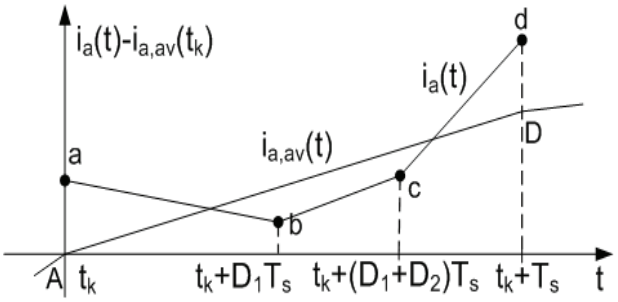

Fig. 10. Piece wise linear approximation of average and actual current within one switching period for three-phase circuit

The piece wise linear functions shown in Fig. 10 can be analyzed like in the single phase case (Fig. 3) and the magnitude of ripple function can be determined. The maximum value of ripple function in the switching period starting at t_k and associated with *n*th sector of vector space can be expressed as follows

$$\Delta i_p(t_k) = \frac{V_{Cav}(t_k)T_s}{3L}[(s_{1np} - s_{pav})(D_{1n}^2 + 2D_{1n}D_{2n} + 2D_{1n}D_{3n}) + (s_{2np} - s_{pav})(D_{2n}^2 + 2D_{2n}D_{3n}) + (s_{3np} - s_{pav})D_{3n}^2] \quad (34)$$

for $p = \alpha, \beta$.

The ripple function (34) may be positive or negative. The ripple magnitude can be defined as absolute value of these functions. Because

$$s_{1np}D_{1n} + s_{2np}D_{2n} + s_{a3p}D_{3n} = s_{p,av} \text{ for } p = \alpha, \beta \quad (35)$$

the following relation is true

$$\Delta i_p(t_k) = \Delta i_p(t_k + T_s) \quad \text{for } p = \alpha, \beta \quad (36)$$

Example – fifth order harmonic generation in the three-phase circuit

Assume that fifth order harmonic should be generated in the circuit shown in Fig. 8. The result presented in Fig. 11 has been obtained for the following circuit parameters: $e_a = 600\sin(314t)$ and generator is symmetrical, $L = 10$ mH, $R = 0.08\Omega$, C=50 μF, the capacitor is shunted with conductance $G = 0.0001\frac{1}{\Omega}$, capacitor voltage $V_C = 1000$ V.

The assumed currents to be generated are

$$i_a(t) = 20\sin(5 \cdot 314t) + 0.3\sin(314t)$$
$$i_b(t) = 20\sin(5 \cdot 314t + 2\pi/3) + 0.3\sin(314t - 2\pi/3)$$
$$i_c(t) = 20\sin(5 \cdot 314t - 2\pi/3) + 0.3\sin(314t + 2\pi/3)$$

The fundamental harmonic has to be added in order to ensure the energy balance.

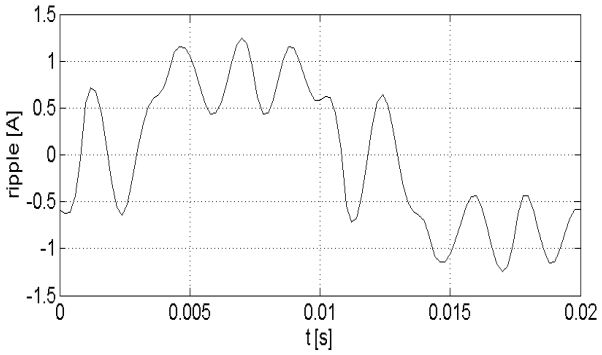

Fig. 11 . Ripple magnitude when fifth order harmonic is generated

The ripple magnitude of current shown in Fig. 11 has been computed according to equation (43).

Conclusions

The current ripples can be computed by simulation of a specific PWM realisation. More general information can be obtained from analytical formulae. The average technique is very convenient tool to analyze a behavior of ripples within a switching process. Such analysis is useful for a switching frequency optimization

REFERENCES

[1] X. Mao, R. Ayyanar, H. K. Krishnamurthy, Optimal Variable switching Frequency Scheme for Reducing Switching Loss in Single – Phase Inverters Based on Time – Domain Ripple Analysis, IEEE Trans. Power Electron., vol. 24, No. 4, pp. 991-1001, 2009

[2] M. Tavakoli Bina, Ashoka K. S. Bhat, Averaging Technique for the Modeling of STATCOM and Active Filters, IEEE Trans. Power Electron., vol. 23, No. 2, pp. 723-734, 2008

[3] K. Mikołajuk, A. Toboła, Average Time-varying Models of Active Power Filters, Przegląd Elektrotechniczny, No. 1, 2010, pp.53-55

***Authors**: prof. dr hab. inż. Kazimierz Mikołajuk, Warsaw University of Technology, ul. Koszykowa 75, 00-661 Warsaw, E-mail: mik@iem.pw.edu.pl; mgr inż. Andrzej Toboła, Warsaw University of Technology, ul. Koszykowa 75, 00-661 Warsaw, E-mail: ato@iem.pw.edu.pl*